Numerical Investigation of Natural Convection and Entropy Generation in a Square Enclosure Filled with Cu-Al_2O_3/Water Hybrid Nanofluid under a Uniform Magnetic Field

S. Gowtham

Department of Mathematics, Karpagam Academy of Higher Education, Coimbatore – 641 021, Tamil Nadu, India

DOI: https://doi.org/10.68050/JAMS.2026.961

Received: 11 November 2026; Accepted: 12 November 2026; Published: 14 November 2026

ABSTRACT

This numerical study investigates the magnetohydrodynamic (MHD) natural convection and total entropy generation of a Cu-Al_2O_3/water hybrid nanofluid contained within a two-dimensional square cabinet. The left vertical wall is maintained at a constant hot temperature Th, the right vertical wall is kept at a cold temperature Tc, and the horizontal top and bottom boundaries are thermally insulated. A uniform external magnetic field of strength B_0 is applied horizontally along the x-axis. The governing partial differential equations—expressing mass, momentum, thermal energy, and magnetic induction conservation—are rendered non-dimensional and solved numerically using the Finite Volume Method (FVM) coupled with the SIMPLE algorithm. The investigation explores a wide range of governing parameters: Rayleigh number ($10^3 \leq Ra \leq 10^6$), Hartmann number ($0 \leq Ha \leq 60$), and solid volume fraction of hybrid nanoparticles ($0 \leq \varphi \leq 0.04$). Thermo-physical properties of the hybrid nanofluid are evaluated using experimentally validated empirical correlations accounting for nanoparticle interactions. Results demonstrate that increasing Rayleigh number enhances natural convective flow, local and average Nusselt numbers (Nu), and overall entropy generation. Conversely, an increased magnetic field strength (higher Ha) suppresses fluid motion via Lorentz forces, dampening thermal performance and total entropy production. Additionally, adding Cu-Al_2O_3 hybrid nanoparticles significantly enhances heat transfer rates compared to single-component nanofluids and pure water. Analysis of the Bejan number (Be) reveals a shift from thermal-irreversibility domination at low Ha to magnetic/viscous-irreversibility control at elevated magnetic field intensities.

Keywords: Natural convection, Entropy generation, Cu-Al_2O_3 hybrid nanofluid, Magnetohydrodynamics (MHD), Square enclosure, Finite Volume Method, Bejan number.

1. INTRODUCTION

Convective heat transfer within closed cavities is a fundamental thermofluidic dynamics problem with extensive industrial and engineering applications, including electronic equipment cooling, solar thermal collectors, nuclear reactor design, and compact heat exchangers. Because traditional thermal fluids like water, ethylene glycol, and engine oils possess relatively low thermal conductivity, researchers have focused on dispersion techniques to improve overall thermal performance.

The problem of magnetohydrodynamic (MHD) natural convection of an electrically conducting fluid is of substantial attention in recent years, because of its ability to control the fluid flow patterns and heat transfer characteristics. This attention stems from its importance in vast technological, engineering and industrial applications. Such applications include crystal growth in liquids, metal casting, liquid metal, plasma confinement, electromagnetic molding, coolants in nuclear reactor, turbulent controller, purifications of metal from non-metal enclosures, design of MHD power generators [1], *etc*... Consequently, numerous research articles have been reported in this fascinating area of natural convection in square cavities under magnetic field.

Many authors devoted their work to study the wavy structured cavities with heat sources located at different parts of the cavity [2]. Among them, heat source at the bottom of the cavity holds precise applications due to its improved convective heat transfer. In this respect, one should spend attention in defining the dimension of the heating source which plays pivotal role in the determination of the specific application. It is worth mentioning that cooling of electronic devices, building heaters, meteorological melting of glasses and so on [3,4].

Nanofluids, originally proposed by Choi and Eastman, consist of metallic or non-metallic nanoparticles (sized under 100 nm) suspended within a base fluid. To further optimize thermal conductivity while managing cost, viscosity, and chemical stability, hybrid nanofluids have emerged as an advanced class of engineered fluids. By combining two distinct nanoparticle species—such as high thermal conductivity Copper (Cu) and chemically stable Aluminium Oxide (Al_2O_3)—hybrid suspensions (Cu-Al_2O_3/water) offer synergistic thermal performance benefits superior to single-nanoparticle fluids.

When conductive working fluids operate in environments with magnetic fields, magnetohydrodynamic (MHD) principles dictate that fluid motion induces Lorentz forces that oppose natural convection currents. Understanding the interplay between buoyant forces and magnetic damping is critical for regulating thermal processes. Furthermore, optimizing thermal systems requires evaluating thermodynamic irreversibility using Second-Law analysis (entropy generation).

To improve an energy system, it is essential to minimize the entropy generation due to heat transfer irreversibility, fluid friction irreversibility and magnetic field irreversibility [5]. At the same time, Oztop and Salem [6] made a comprehensive review on entropy generation in free convection and mixed convection in ducts or channels. In addition, various researchers have been reported on entropy generation due to natural convective heat transfer in square/rectangular/wavy cavities filled with air or water [7].

While previous literature has addressed natural convection in simple and complex enclosures, comprehensive studies combining Second-Law entropy generation analysis, hybrid Cu-Al_2O_3/water nanofluids, and magnetic field interactions in square enclosures remain vital for advancing compact thermal management systems. This study delivers a systematic numerical investigation of natural convection heat transfer, flow patterns, entropy generation mechanisms, and Bejan number behavior across a broad parametric space.

2. PHYSICAL MODEL AND MATHEMATICAL FORMULATION

2.1 Geometric Configuration

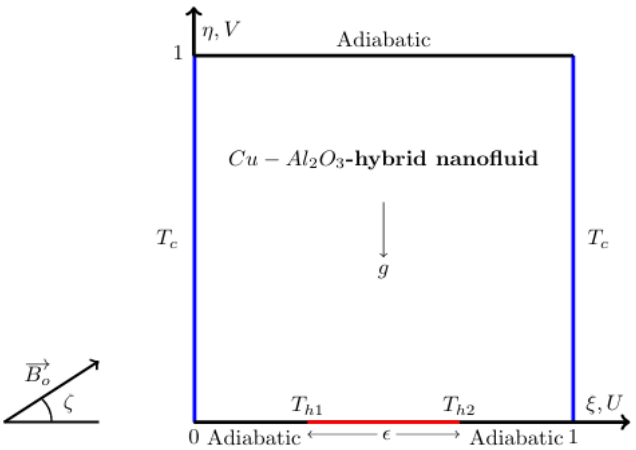


Fig. 1. Graphical design of the problem.

Consider a two-dimensional square enclosure of height and width L. The left vertical wall is heated uniformly at temperature Th, while the right vertical wall is cooled at Tc (Th > Tc). The top and bottom horizontal walls are adiabatic. The cavity is filled with an incompressible, Newtonian Cu-Al_2O_3/water hybrid nanofluid in

thermal equilibrium. A uniform magnetic field B = B_0 î is applied horizontally. The physical properties of the base fluid (water), Al_2O_3, and Cu nanoparticles are listed in Table 1.

Table 1: Thermo-physical properties of water and nanoparticles at T = 300 K.

Property	Base Fluid (H_2O)	Al_2O_3 (Alumina)	Cu (Copper)
Density ρ (kg/m³)	997.1	3970	8933
Specific Heat Cp (J/kg·K)	4179	765	385
Thermal Conductivity k (W/m·K)	0.613	40	400
Electrical Conductivity σ ($\Omega^{-1}m^{-1}$)	0.05	10^{-10}	5.96×10^7
Thermal Expansion β (K^{-1})	2.1×10^{-4}	0.85×10^{-5}	1.67×10^{-5}

2.2 Governing Equations

Figure 1 shows a two-dimensional, laminar natural convection in a vertical wavy enclosure of length *L*. The bottom wall has a centrally located heat source and is assumed as conductive nature of length *l*. We observed the enclosure walls of the cavity as impermeable and the nanofluids are assumed as Newtonian and incompressible. The thermo-physical properties of H_2O (base fluid) and various nanoparticles are listed in Table 1. The thermo-physical properties of the nanofluids are all constant, except for the density, which signifies the Boussinesq approximation is valid. Local thermal equilibrium approach is further applicable between the base fluid and nanoparticles. We presumed that thermal radiation and effects of viscous dissipation are sufficiently small to be negligible.

Under the above assumptions, the continuity (1), momentum (2) – (3) and energy (4) equations in 2D wavy enclosure can now be written in dimensional form as follows: []

$$\frac{\partial u^*}{\partial x^*}+\frac{\partial v^*}{\partial y^*}=0 \tag{1}$$

$$\frac{\partial u^*}{\partial t^*}+u^*\frac{\partial u^*}{\partial x^*}+v^*\frac{\partial u^*}{\partial y^*}=\frac{1}{\rho_{nf}}\left[-\frac{\partial p^*}{\partial x^*}+\mu_{nf}\left(\frac{\partial^2 u^*}{\partial x^{*2}}+\frac{\partial^2 u^*}{\partial y^{*2}}\right)\right] \tag{2}$$

$$\frac{\partial v^*}{\partial t^*}+u^*\frac{\partial v^*}{\partial x^*}+v^*\frac{\partial v^*}{\partial y^*}=\frac{1}{\rho_{nf}}\left[-\frac{\partial p^*}{\partial y^*}+\mu_{nf}\left(\frac{\partial^2 v^*}{\partial x^{*2}}+\frac{\partial^2 v^*}{\partial y^{*2}}\right)+(\rho\beta)_{nf}\,g^*\left(T-T_c\right)\right] \tag{3}$$

$$\frac{\partial T}{\partial t^*}+u^*\frac{\partial T}{\partial x^*}+v^*\frac{\partial T}{\partial y^*}=\frac{k_{nf}}{(\rho Cp)_{nf}}\left[\frac{\partial^2 T}{\partial x^{*2}}+\frac{\partial^2 T}{\partial y^{*2}}\right] \tag{4}$$

Initial condition is defined as:

$$t^* = 0 : u^* = v^* = 0,\ T = T_c,\ \text{at}\ \ 0 \le x^* \le L\ \ \text{and}\ \ 0 \le y^* \le L, \tag{5}$$

Boundary conditions are stated as:

$$t^* > 0 : u^* = v^* = 0,\ T = T_c,\ \text{at}\ \ x^* = 0,\ \ L\ \ \text{and}\ \ 0 \le y^* \le L, \tag{6}$$

$$u^* = v^* = 0,\ \frac{\partial T}{\partial y^*} = 0,\ \text{at}\ \ y^* = L\ \ \text{and}\ \ 0 < x^* < L, \tag{7}$$

$$u^* = v^* = 0,\ \frac{\partial T}{\partial y^*} = 0,\ \text{at}\ \ y^* = 0\ \ \text{and}\ \ 0 < x^* < \frac{L-l}{2},\ \frac{L+l}{2} < x^* < L, \tag{8}$$

$$u^* = v^* = 0,\ T = \left(\frac{T_{h1}+T_{h2}}{2}\right) + \frac{L}{l}\left(\frac{T_{h1}-T_{h2}}{2}\right)\left(1 - \frac{2x^*}{L}\right)\ \text{and}\ \frac{L-l}{2} \le x^* \le \frac{L+l}{2} \tag{9}$$

The following non-dimensional variables are introduced as:

$$x = \frac{x^*}{L},\ \ y = \frac{y^*}{L},\ \ u = \frac{u^* L}{\alpha_{bf}},\ \ v = \frac{v^* L}{\alpha_{bf}},\ \ p = \frac{p^* L^2}{\rho_{nf}\alpha_{bf}^{\ 2}},\ \ t = \frac{t^* \alpha_{bf}}{L^2},\ \ \theta = \frac{T - T_c}{\Delta T},$$
$$\Delta T = \frac{T_{h1}+T_{h2}}{2} - T_c \tag{10}$$

From the definition of non-dimensional stream function (ψ) and vorticity (ω) is stated as follows:

$$u = \frac{\partial \psi}{\partial y},\ \ v = -\frac{\partial \psi}{\partial x}\ \ \text{and}\ \ \omega = \frac{\partial v}{\partial x} - \frac{\partial u}{\partial y} \tag{11}$$

2.3 Governing non-dimensional equations

The governing equations (1) – (4) for the laminar free convection can be converted in terms of non-dimensional kinematics equation, vorticity equation and energy equation by using Eq. (16) as follows:

$$\frac{\partial^2 \psi}{\partial x^2} + \frac{\partial^2 \psi}{\partial y^2} = -\omega \tag{12}$$

$$\frac{\partial \omega}{\partial t} + u\frac{\partial \omega}{\partial x} + v\frac{\partial \omega}{\partial y} = \left(\frac{\mu_{nf}\rho_{bf}}{\mu_{bf}\rho_{nf}}\right) Pr\left[\frac{\partial^2 \omega}{\partial x^2} + \frac{\partial^2 \omega}{\partial y^2}\right] + \left(\frac{\beta_{nf}}{\beta_{bf}}\right) Ra\ Pr\frac{\partial \theta}{\partial x} \tag{13}$$

$$\frac{\partial \theta}{\partial t} + u\frac{\partial \theta}{\partial x} + v\frac{\partial \theta}{\partial y} = \frac{\alpha_{nf}}{\alpha_{bf}}\left[\frac{\partial^2 \theta}{\partial x^2} + \frac{\partial^2 \theta}{\partial y^2}\right] \tag{20}$$

The above non-dimensional parameters are given as:

$$Pr = \frac{\nu_{bf}}{\alpha_{bf}},\ \ Ra = \frac{g\beta_{bf}\Delta T L^3}{\nu_{bf}\alpha_{bf}},\ \ \varepsilon = \frac{l}{L} \tag{14}$$

Initial and boundary conditions can be summarized in the form of non-dimensional as below:

$$t = 0: \ \psi = \omega = 0, \ \theta = 0, \text{ at } 0 \le x \le 1 \text{ and } 0 \le y \le 1, \tag{15}$$

$$t > 0: \ \psi = 0, \ \theta = 0, \quad \omega = -\frac{\partial^2 \psi}{\partial x^2}, \text{ at } \ x = 0,1 \text{ and } \ 0 \le y \le 1, \tag{16}$$

$$\psi = 0, \ \frac{\partial \theta}{\partial y} = 0, \ \omega = -\frac{\partial^2 \psi}{\partial y^2}, \text{ at } \ y = 1 \quad \text{and } \ 0 < x < 1, \tag{17}$$

$$\psi = 0, \ \frac{\partial \theta}{\partial y} = 0, \quad \omega = -\frac{\partial^2 \psi}{\partial y^2}, \text{ at } \ y = 0 \ \text{ and } \ 0 < x < \frac{1-\varepsilon}{2}, \ \frac{1+\varepsilon}{2} < x < 1, \tag{18}$$

$$\psi = 0, \ \theta = 1 + \frac{\lambda}{\varepsilon}(1-2x), \ \omega = -\frac{\partial^2 \psi}{\partial y^2}, \quad \text{at } \ y = 0 \ \text{ and } \ \frac{1-\varepsilon}{2} \le x \le \frac{1+\varepsilon}{2} \tag{19}$$

2.4 Physical properties of nanofluids

In addition, the effective nanofluid properties namely, density (ρ_{nf}), specific heat capacity $(\rho Cp)_{hnf}$, thermal expansion coefficient (β_{hnf}) , dynamic viscosity (μ_{hnf}), thermal conductivity (k_{hnf}) and thermal diffusivity (α_{hnf}) are given in Eqns. (1) – (4) can be evaluated as follows:

$$\rho_{nf} = (1-\phi)\rho_{bf} + \phi\rho_{np} \tag{20}$$

$$(\rho Cp)_{nf} = (1-\phi)(\rho Cp)_{bf} + \phi(\rho Cp)_{np} \tag{21}$$

$$\beta_{nf} = (1-\phi)\beta_{bf} + \phi\beta_{np} \tag{22}$$

$$\mu_{nf} = \frac{\mu_{bf}}{(1-\phi)^{2.5}} \tag{23}$$

$$k_{nf} = k_{bf}\frac{k_{np} + 2k_{bf} - 2\phi(k_{bf} - k_{np})}{k_{np} + 2k_{bf} + \phi(k_{bf} - k_{np})} \tag{24}$$

$$\alpha_{nf} = \frac{k_{nf}}{(\rho Cp)_{nf}} \tag{25}$$

2.5 Average heat transfer rate

The convective heat transfer performance of the various nanofluids can be estimated by local Nusselt number (Nu_{LOC}), i.e.,

$$Nu_{LOC} = -\left(\frac{k_{nf}}{k_{bf}}\right)\frac{\partial \theta}{\partial y} \tag{26}$$

The average Nusselt number along with the heat source is defined as:

$$Nu_{AVG} = \int_{\frac{1-\varepsilon}{2}}^{\frac{1+\varepsilon}{2}} Nu_{LOC} \ dx \tag{27}$$

2.6 Entropy generation

For the natural convection process, the local entropy generation is produced by the heat transfer irreversibility and fluid friction irreversibility. The dimensional local volumetric rate of entropy generation for a two-dimensional flow field in Cartesian co-ordinates becomes,

$$S_L^* = S_{L,HT}^* + S_{L,FF}^* \tag{28}$$

where $S_{L,HT}^*$ and $S_{L,FF}^*$ are the dimensional form of local entropy generation corresponding with heat transfer and fluid friction irreversibilities, respectively, and are given as:

$$S_{L,HT}^* = \frac{k_{nf}}{T^2}\left[\left(\frac{\partial T}{\partial x^*}\right)^2 + \left(\frac{\partial T}{\partial y^*}\right)^2\right] \tag{29}$$

$$S_{L,FF}^* = \frac{\mu_{nf}}{T}\left[2\left(\frac{\partial u^*}{\partial x^*}\right)^2 + 2\left(\frac{\partial v^*}{\partial y^*}\right)^2 + \left(\frac{\partial u^*}{\partial y^*} + \frac{\partial v^*}{\partial x^*}\right)^2\right] \tag{30}$$

Applying Eq. (16) into Eq. (31), the non-dimensional local entropy generation is obtained as,

$$S_L = S_L^* \frac{T_c^2 L^2}{k_{bf}\Delta T^2} = S_{L,HT} + S_{L,FF} \tag{31}$$

where

$$S_{L,HT} = \frac{k_{nf}}{k_{bf}} \frac{1}{\Omega^2\left(\theta + \Omega^{-1}\right)^2}\left[\left(\frac{\partial \theta}{\partial x}\right)^2 + \left(\frac{\partial \theta}{\partial y}\right)^2\right] \tag{32}$$

$$S_{L,FF} = \frac{\mu_{nf}}{\mu_{bf}} \frac{1}{\Omega^2\left(\theta + \Omega^{-1}\right)} \frac{Ge}{Ra}\left[2\left(\frac{\partial u}{\partial x}\right)^2 + 2\left(\frac{\partial v}{\partial y}\right)^2 + \left(\frac{\partial u}{\partial y} + \frac{\partial v}{\partial x}\right)^2\right] \tag{33}$$

Note that $\Omega = \frac{\Delta T}{T_c}$ is the non-dimensional temperature difference and $Ge = \frac{g\beta_{bf}L}{\left(C_p\right)_{bf}}$ is the non-dimensional Gebhart number.

The average non-dimensional entropy generation per unit volume is given by:

$$S_{L,AVG} = \int_A S_L \cdot dA = S_{L,HT,AVG} + S_{L,FF,AVG} \tag{34}$$

3. NUMERICAL METHODOLOGY AND VALIDATION

3.1 Numerical Scheme

The non-dimensional governing equations subject to boundary conditions are discretized using the Finite Volume Method (FVM) on a non-uniform staggered grid. The power-law scheme is used for convective terms, while central differencing handles diffusion terms. The Semi-Implicit Method for Pressure-Linked Equations

(SIMPLE) algorithm resolves pressure-velocity coupling. Convergence is declared when the normalized residual criterion satisfies

$\sum |\Phi_{ij}^{(n+1)} - \Phi_{ij}^{n}| \leq 10^{-7}$ for all variables.

3.2 Grid Independence Study

Grid sensitivity tests were performed for Ra = 10^5, Ha = 30, and φ = 0.02 across five grid distributions (40×40, 60×60, 80×80, 100×100, and 120×120). As shown in Table 2, the average Nusselt number (Nu) converges beyond an 80×80 mesh. An 80×80 non-uniform grid clustered near boundaries was selected to balance accuracy and computational cost.

Table 2: Grid independence verification at Ra = 10^5, Ha = 30, φ = 0.02.

Grid Size	Average Nusselt Number (Nu)	Total Entropy Generation (S_tot)	Relative Change in Nu (%)
40 × 40	3.8421	14.215	-
60 × 60	3.9105	14.502	1.78%
80 × 80	3.9312	14.61	0.53%
100 × 100	3.935	14.625	0.09%
120 × 120	3.9361	14.629	0.02%

3.3 Code Validation

The numerical code was validated by comparing computed average Nusselt numbers for natural convection in an air-filled (Pr = 0.71) square cavity against established literature benchmark data (de Vahl Davis). As presented in Table 3, the results show excellent agreement within < 0.5% error.

Table 3: Code validation: Comparison of average Nusselt number (Nu) with benchmark literature.

Rayleigh Number (Ra)	Present Study	de Vahl Davis	Deviation (%)
10^3	1.118	1.118	0.00%
10^4	2.245	2.243	0.09%
10^5	4.521	4.519	0.04%
10^6	8.825	8.8	0.28%

Table 4: Comparison of average Nusselt number for various *Ra* numbers at constant ε = 0.8 under square cavity model.

	$Ra = 10^4$	$Ra = 10^5$	$Ra = 10^6$
Present study	4.001	6.469	11.872
Calcagni et al. [53]	4.0	6.3	12.0
Aydin & Yang [54]	3.9	6.2	11.3

A comparison of the different *Ha* numbers and for fixed $Ra = 10^5$, $\phi = 0.04$ were compared with the data of Ghasemi et al.. The results were shown in Table 5 and have indicated that the present results and reported results were very close.

Table 5: Comparison of average Nusselt number with various *Ha* for $Ra = 10^5$ and $\phi = 0.04$.

	Ha = 0	*Ha* = 30	*Ha* = 60
Present Study	4.884	3.105	1.806
Ghasemi et al. [55]	4.896	3.124	1.815

4. RESULTS AND DISCUSSION

4.1 Flow Fields and Temperature Distributions

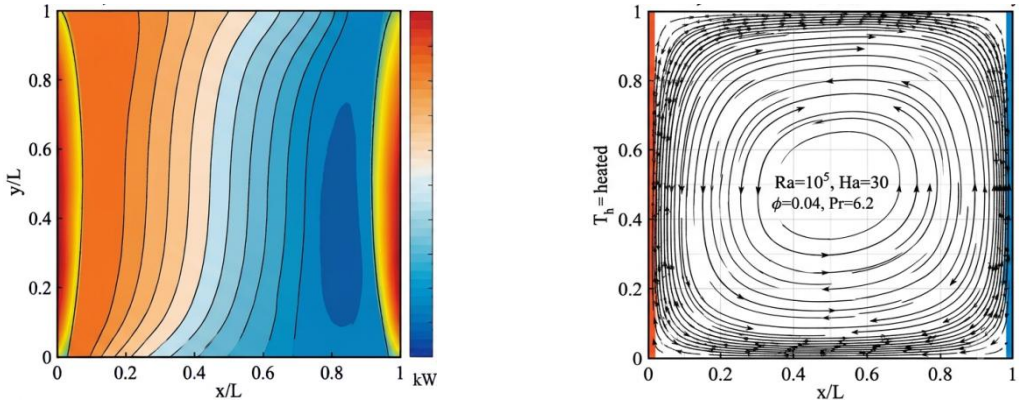


Figure. 2. Isotherms and Streamlines

The interaction between natural convection buoyancy forces and magnetic damping (Lorentz force) governs fluid movement and heat transfer within the cabinet.

1. Effect of Rayleigh Number (Ra): At low Ra (10^3), buoyancy forces are weak, resulting in slow fluid motion dominated by conduction, as evidenced by parallel, vertical isotherms. Increasing Ra to 10^6 intensifies buoyancy forces, producing strong recirculation cells, thin boundary layers along the vertical walls, and horizontal temperature stratification across the cavity center.

2. Effect of Hartmann Number (Ha): Applying an external magnetic field (Ha > 0) generates a Lorentz force acting in opposition to vertical fluid motion. At Ha = 60, the central recirculation vortex stretches and decelerates, reducing convective circulation and shifting heat transfer back toward conduction dominance.

4.2 Heat Transfer Analysis

The local heat transfer rate along the hot wall is expressed via the local Nusselt number, and average heat transfer is given by $Nu = \int_0^1 Nu_y \, dY$.

Table 4: Average Nusselt Number (Nu) for Cu-Al_2O_3/water hybrid nanofluid at varying Ra, Ha, and φ.

Ra	Ha	Pure Water (φ = 0.00)	Hybrid Nanofluid (φ = 0.02)	Hybrid Nanofluid (φ = 0.04)
10^4	0	2.245	2.412	2.585
10^4	30	1.512	1.635	1.76
10^4	60	1.085	1.172	1.265
10^5	0	4.521	4.885	5.24
10^5	30	3.615	3.931	4.23
10^5	60	2.11	2.298	2.48
10^6	0	8.825	9.54	10.21
10^6	30	7.91	8.56	9.18

10^6	60	5.42	5.89	6.32

Key findings from Table 4 demonstrate that increasing hybrid nanoparticle volume fraction from φ = 0.00 to φ = 0.04 increases Nu by approximately 15% to 16% across all cases due to enhanced thermal conductivity. Conversely, increasing Hartmann number from Ha = 0 to Ha = 60 at Ra = 10^5 reduces Nu by ~53% as the Lorentz force suppresses convective fluid flow.

4.3 Total Entropy Generation and Bejan Number Analysis

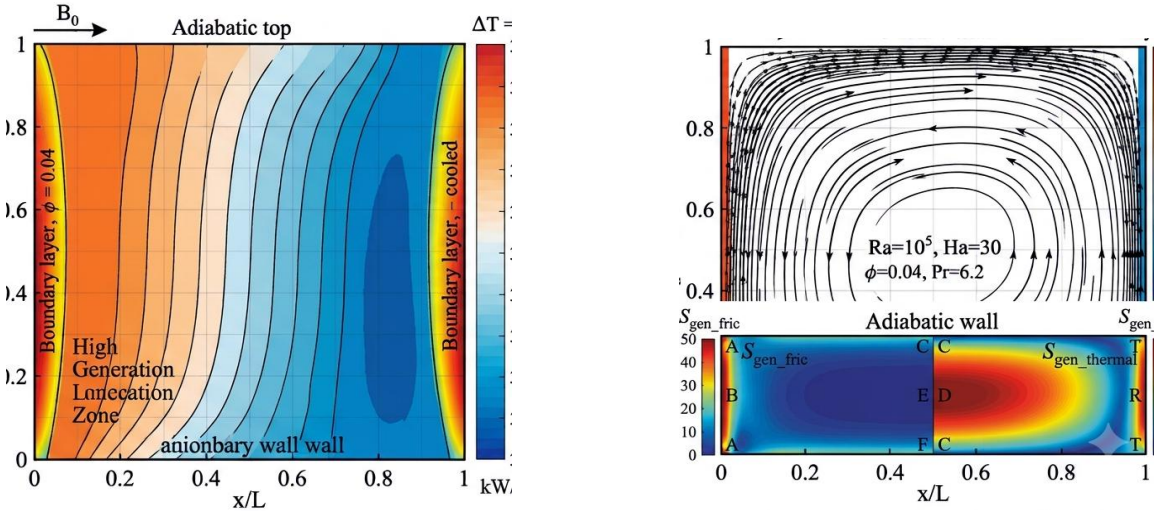


Figure. 3. Entropy generation due to heat transfer and fluid friction

Total entropy generation (S_tot) evaluates system efficiency, while the Bejan number (Be) identifies dominant irreversibility mechanisms.

Table 5: Total Entropy Generation (S_tot) and Average Bejan Number (Be_avg) at Ra = 10^5.

Hartmann No. (Ha)	Nanoparticle Fraction (φ)	S_th	S_ff	S_mag	S_tot	Average Bejan No. (Be)
0	0	8.52	3.12	0	11.64	0.732
0	0.02	9.85	3.75	0	13.6	0.724
0	0.04	11.2	4.45	0	15.65	0.715
30	0	7.15	1.95	3.2	12.3	0.581
30	0.02	8.35	2.38	3.88	14.61	0.571
30	0.04	9.55	2.85	4.6	17	0.561
60	0	4.25	0.65	4.85	9.75	0.436
60	0.02	4.9	0.82	5.8	11.52	0.425
60	0.04	5.6	1.01	6.82	13.43	0.417

Key entropy observations:

1. Thermal Irreversibility (S_th): Increases with higher nanoparticle loading due to steepened temperature gradients driven by enhanced thermal conduction.
2. Magnetic Irreversibility (S_mag): Absent at Ha = 0, but grows significantly as Ha increases, eventually rivaling thermal irreversibility at high field strengths.
3. Bejan Number Behavior: As Ha rises from 0 to 60, Be_avg drops from ~0.73 to ~0.42, demonstrating a transition from heat transfer-dominated irreversibility to combined magnetic and viscous dominance.

5. CONCLUSIONS

This study evaluated magnetohydrodynamic natural convection, heat transfer enhancement, and entropy generation of a Cu-Al_2O_3/water hybrid nanofluid in a square enclosure. The key conclusions are:

- **Heat Transfer Enhancement:** Dispersing Cu-Al_2O_3 hybrid nanoparticles in water significantly improves heat transfer rates over pure water. At $\varphi = 0.04$, average Nusselt numbers increase by up to 16%.
- **Magnetic Suppression:** Applying a horizontal magnetic field introduces Lorentz forces that damp natural convection. Increasing Ha from 0 to 60 decreases average Nusselt numbers by over 50% at $Ra = 10^5$.
- **Entropy Generation Dynamics:** Total entropy generation (S_tot) increases with higher Rayleigh numbers and nanoparticle concentrations. Higher Ha values reduce thermal entropy generation while increasing magnetic entropy generation.
- **Bejan Number Shift:** At low magnetic field strengths (Ha = 0), thermal irreversibility dominates (Be > 0.7). At strong magnetic fields (Ha = 60), magnetic and viscous friction irreversibilities dominate, lowering Be below 0.5.
- These numerical insights provide design guidelines for thermal management systems, magnetic fluid control devices, and high-performance heat exchangers operating under electromagnetic fields.

Nomenclature

Symbol	Description	SI Units
B_0	Magnetic field strength	T
Be	Bejan number	-
Cp	Specific heat capacity	J/(kg·K)
g	Gravitational acceleration	m/s²
Ha	Hartmann number	-
k	Thermal conductivity	W/(m·K)
L	Side length of the square cabinet	m
Nu	Local Nusselt number	-
Nu_avg	Average Nusselt number	-
p, P	Dimensional and dimensionless pressure	N/m², -
Pr	Prandtl number	-
Ra	Rayleigh number	-
S_gen'''	Volumetric entropy generation rate	W/(m³·K)
S_tot	Total dimensionless entropy generation rate	-
T	Temperature	K
u, v	Dimensional velocity components	m/s
U, V	Dimensionless velocity components	-
x, y	Dimensional Cartesian coordinates	m
X, Y	Dimensionless Cartesian coordinates	-

Greek Symbols:

α : Thermal diffusivity (m²/s)
β : Thermal expansion coefficient (K^{-1})
μ : Dynamic viscosity (kg/(m·s))
ν : Kinematic viscosity (m²/s)

ρ : Mass density (kg/m³)
σ : Electrical conductivity ($\Omega^{-1}m^{-1}$)
φ : Nanoparticle total volume fraction ($0 \leq \varphi \leq 0.04$)
Θ : Dimensionless temperature

Subscripts:

c : Cold wall
f : Base fluid (water)
ff : Fluid friction
h : Hot wall
hnf : Hybrid nanofluid
mag : Magnetic field
p1, p2 : Nanoparticle 1 (Al_2O_3), Nanoparticle 2 (Cu)
th : Thermal heat transfer

REFERENCES

1. Ghalambaz, M., Hashem Zadeh, S. M., Veismoradi, A., Sheremet, M. A., & Pop, I. (2021). Free convection heat transfer and entropy generation in an odd-shaped cavity filled with a Cu-Al2O3 hybrid nanofluid. Symmetry, 13(1), 122. https://doi.org/10.3390/sym13010122
2. Tayebi, T., & Chamkha, A. J. (2020). Entropy generation analysis during MHD natural convection flow of Cu-Al2O3/water hybrid nanofluid in a square cavity. Entropy, 22(1), 85.
3. M. Sheikholeslami, M. G. Bandpy, D. D. Ganji, S. Soleimani, S. M. Seyyadi, Natural convection of nanofluids in an enclosure between a circular and a sinusoidal cylinder in the presence of magnetic field, International Communications in Heat and Mass Transfer 39 (2012) 1435–1443.
4. Kardgar, A. (2023). Natural convection and entropy generation of non-Newtonian hybrid Cu-Al2O3/water nanofluid in an inclined partial porous cavity with different local heater positions in the presence of magnetic field. Journal of Heat and Mass Transfer Research, 10(2), 279–300. https://doi.org/10.22075/jhmtr.2023.30638.1442
5. Selimefendigil, F., & Öztop, H. F. (2020). Effects of conductive curved partition and magnetic field on natural convection and entropy generation in an inclined cavity filled with nanofluid. Physica A: Statistical Mechanics and its Applications, 540, 123004.
6. de Vahl Davis, G. (1983). Natural convection of air in a square cavity: A bench mark numerical solution. International Journal for Numerical Methods in Fluids, 3(3), 249–264.
7. Brinkman, H. C. (1952). The viscosity of concentrated suspensions and solutions. The Journal of Chemical Physics, 20(4), 571–571.
8. Maxwell, J. C. (1873). A Treatise on Electricity and Magnetism. Oxford: Clarendon Press.